GFZ
Helmholtz-Zentrum
POTSDAM

Originally published as:

Melgar, D., Allen, R. M., Riquelme, S., Geng, J., Bravo, F., Baez, J. C., Parra, H., Barrientos, S., Fang, P., Bock, Y., Bevis, M., Caccamise, D. J., Vigny, C., Moreno, M., Smalley, R. (2016): Local tsunami warnings: Perspectives from recent large events. - *Geophysical Research Letters*, *43*, 3, pp. 1109—1117.

DOI: http://doi.org/10.1002/2015GL067100

AGU PUBLICATIONS

Geophysical Research Letters

RESEARCH LETTER
10.1002/2015GL067100

Key Points:
- Local warning within 2–3 min of a large earthquake is possible
- Rapid source models can be used for warning
- This method can be used with current infrastructure

Supporting Information:
- Figures S1–S11

Correspondence to:
D. Melgar,
dmelgar@berkeley.edu

Citation:
Melgar, D., et al. (2016), Local tsunami warnings: Perspectives from recent large events, *Geophys. Res. Lett.*, *43*, 1109–1117, doi:10.1002/2015GL067100.

Received 19 NOV 2015
Accepted 28 DEC 2015
Accepted article online 3 JAN 2016
Published online 12 FEB 2016

©2016. American Geophysical Union. All Rights Reserved.

Local tsunami warnings: Perspectives from recent large events

Diego Melgar[1], Richard M. Allen[1], Sebastian Riquelme[2], Jianghui Geng[3,4], Francisco Bravo[5], Juan Carlos Baez[2], Hector Parra[6], Sergio Barrientos[2], Peng Fang[3], Yehuda Bock[3], Michael Bevis[7], Dana J. Caccamise II[7,8], Christophe Vigny[9], Marcos Moreno[10], and Robert Smalley Jr.[11]

[1]Seismological Laboratory, University of California, Berkeley, California, USA, [2]Centro Sismológico Nacional, Universidad de Chile, Santiago, Chile, [3]Cecil H. and Ida M. Green Institute of Geophysics and Planetary Physics, Scripps Institution of Oceanography, University of California, San Diego, La Jolla, California, USA, [4]GNSS Center, Wuhan University, Wuhan, China, [5]Departamento de Geofísica, Universidad de Chile, Santiago, Chile, [6]Instituto Geográfico Militar, Santiago, Chile, [7]School of Earth Sciences, Ohio State University, Columbus, Ohio, USA, [8]Now at National Geodetic Survey, National Oceanographic and Atmospheric Administration, Silver Spring, Maryland, USA, [9]Laboratoire de Géologie, École Normale Supérieure, Paris, France, [10]Helmholtz Centre, GFZ German Research Centre for Geosciences, Potsdam, Germany, [11]CERI, University of Memphis, Memphis, Tennessee, USA

Abstract We demonstrate a flexible strategy for local tsunami warning that relies on regional geodetic and seismic stations. Through retrospective analysis of four recent tsunamigenic events in Japan and Chile, we show that rapid earthquake source information, provided by methodologies developed for earthquake early warning, can be used to generate timely estimates of maximum expected tsunami amplitude with enough accuracy for tsunami warning. We validate the technique by comparing to detailed models of earthquake source and tsunami propagation as well as field surveys of tsunami inundation. Our approach does not require deployment of new geodetic and seismic instrumentation in many subduction zones and could be implemented rapidly by national monitoring and warning agencies. We illustrate the potential impact of our method with a detailed comparison to the actual timeline of events during the recent 2015 M_w8.3 Illapel, Chile, earthquake and tsunami that prompted the evacuation of 1 million people.

1. Motivation

Compared to other natural hazards, large tsunamis are infrequent, and as a result, local tsunami warning systems are not usually a priority and do not exist in the majority of countries located along subduction zones (including the United States). Recent events in Indonesia, Chile, and Japan, however, have shown that tsunamis can lead to substantial casualties, potentially tallied in the tens to hundreds of thousands of lives, as well as to the total economic collapse of the affected regions [*Athukorala and Resosudarmo*, 2005; *Mimura et al*., 2011]. To compound the problem, population in tsunami-prone areas has steadily increased over the last 25 years [*Center for International Earth Science Information Network (CIESIN) and Centro Internacional de Agricultura Tropical (CIAT),* 2005] (Figure 1a), making it difficult to evacuate large numbers of people from dense population centers in many low-lying coastal areas. Evacuation start time is the most important variable in tsunami mortality rates [*Yun and Hamada*, 2015]; therefore, rapid tsunami information systems that forecast intensities at the regional level are needed to provide actionable information to emergency responders and decision makers to order evacuations in the affected regions as quickly as possible. All of these elements make the development of a rapid and accurate local tsunami warning methodology, and its implementation, a pressing issue.

Currently, after large events, international warning systems rely on teleseismic measurements to estimate an earthquake's size and the propagation of tsunami waves to deep water pressure sensors far from the source area to provide warnings to more distant locations across an ocean basin [*Titov et al*., 2005; *Kumar et al*., 2012; *Hirshorn et al*., 2013]. These far-field measurements are only available after the tsunami has struck the local coastline but can be used for robust basin-scale warnings. Tsunami warning systems such as those operated by Tsunami Warning Centers (TWCs) under the auspices of the U.S. National Oceanographic and Atmospheric Administration (NOAA) rely on these teleseismic measures of earthquake size, *P* wave magnitudes (M_{wp}) and the *W* phase centroid moment tensors [*Hayes et al*., 2011; *Hirshorn et al*., 2013], and on deep water pressure sensors (Deep-ocean Assessment and Reporting of Tsunamis (DART) buoys) that directly measure the

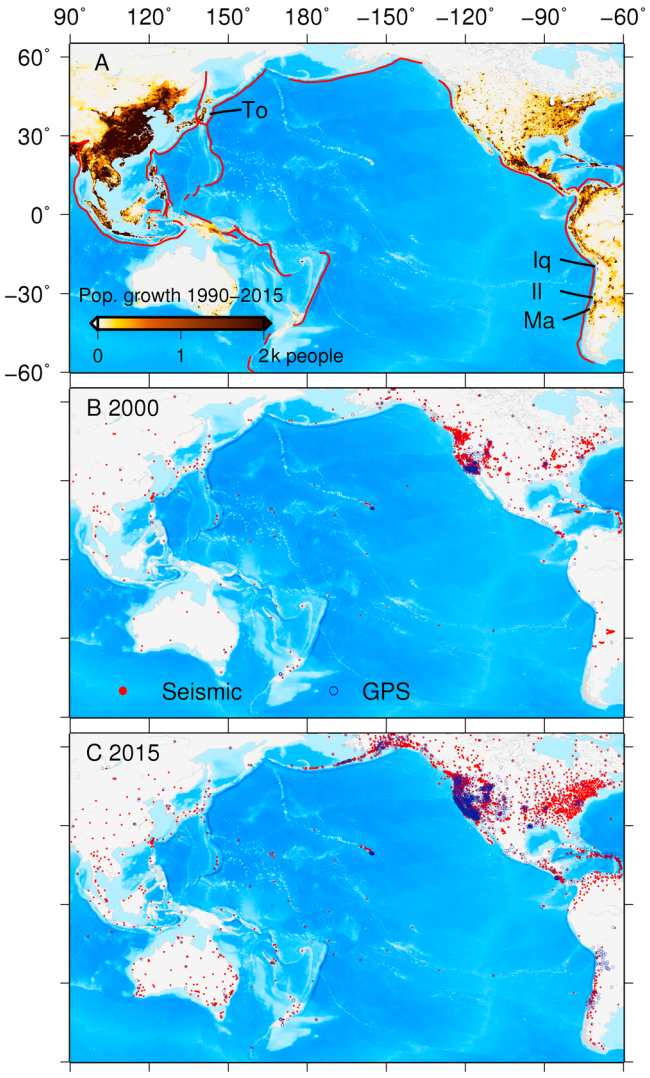

Figure 1. Population growth of the world in the circum-Pacific and Indian Ocean regions and geophysical networks. (a) Population growth between 1990 and 2015 [*CIESIN and CIAT*, 2005]. The red lines indicate subduction zones. The four earthquakes analyzed in this study are labeled as follows: the 2010 Maule, Chile (Ma), 2011 Tohoku-oki, Japan (To), 2014 Iquique, Chile (Iq), and 2015 Illapel, Chile (Il). Seismic and GPS stations reporting to public archives (UNAVCO Inc. and Incorporated Research Institutions for Seismology (IRIS)) (b) in 2000 and (c) in 2015. These stations are representative of the worldwide growth and distribution of geophysical instruments but are not the total number of available stations. Many other stations belong to national and other networks, which are not always publicly available.

tsunami [*Titov et al.*, 2005]. The NOAA system routinely, and very successfully, provides warnings at large distances (~1000 km) from significant earthquakes and across ocean basins. The ability of this system to issue local tsunami warnings, that is, at the coast adjacent to a large earthquake, is limited to certain domestic regions. In contrast, the Japanese Meteorological Agency (JMA) operates an independent system that issues countrywide alerts to the near-source coastline of the Japanese archipelago in the first minutes after an earthquake [*Tatehata*, 1997; *Hoshiba and Ozaki*, 2014]. Their approach relies on rapid magnitude and hypocenter estimates from land-based seismic data. Once these two parameters are available, a database query of precomputed tsunami scenarios is used to identify the scenario with the most similar location and magnitude. An alert is then issued to the near-source coastline based on the precomputed predicted tsunami runups. This warning paradigm was chosen because at the time of its inception more complete characterization of the seismic source and calculation of tsunami propagation—all in real time—was deemed too computationally costly and thus unfeasible [*Tatehata,* 1997]. However, during the 2011 M_w9.0 Tohoku-oki earthquake, the earthquake magnitude was severely underestimated and so the zones of evacuation were not wide enough and may have resulted in higher casualties [*Yun and Hamada*, 2015]. A similar system is now operational in Indonesia [*Lauterjung et al.*, 2014] and has been proposed for Australia [*Allen and Greenslade*, 2008]. These approaches while able to cover the local coast can be hindered by the approximate characterization of the source, the incompleteness of the scenario events in the database, and the overdependence on seismic data that can be unreliable for magnitude assessments in the near field of large events [*Melgar et al.*, 2015].

As populations have grown and technology improved, the number of seismic and geodetic (GPS) sensors across subduction zones has increased as well (Figures 1b and 1c). Many of these sensors are operated by national monitoring agencies that routinely produce a suite of rapid earthquake information products. These range from simple location and magnitude estimates to more complex source products such as regional centroid moment tensors (CMTs) that indicate the style of faulting, or more advanced slip inversions

that reveal the pattern of heterogeneous slip on an assumed fault surface. Many of these networks are also delivering or experimenting with earthquake early warning [*Allen et al*., 2009].

Here we propose and demonstrate a flexible local tsunami warning strategy, which we call T-larms, that harnesses the growth of monitoring infrastructure to produce rapid and effective warning. We show that land-based measurements of the earthquake from local seismic and geodetic stations, coupled with new algorithms to characterize the event, can be used to produce rapid tsunami warning maps for the local coast within 2–3 min after the onset of rupture (Figure S1 in the supporting information) and in advance of the tsunami arrival. Through retrospective analysis of data collected in real time for four recent large events in Japan and Chile, we find that earthquake source information from local stations can be used to produce accurate enough estimates of maximum expected tsunami amplitude as to be useful for warning. We emphasize the comparison between our approach and the timeline of response during 2015 M_w8.3 Illapel, Chile, earthquake and tsunami during which 1 million people were evacuated. We demonstrate the speedup in region-specific tsunami intensity estimation from 31 to 3 min for that event. Our results show that local tsunami warning is possible with the currently available seismic and geodetic infrastructure in many subduction zones around the world. National monitoring and warning agencies could rapidly implement our approach to improve situational awareness, thereby potentially saving many thousands of lives in the coming years.

2. Analysis Method and Data

We retrospectively analyze seismic and geodetic data collected during the 2010 M_w8.8 Maule, Chile, 2011 M_w9.0 Tohoku-oki, Japan, 2014 M_w8.2 Iquique, Chile, and 2015 M_w8.3 Illapel, Chile, earthquakes (Figures 1 and 2). We consider several types of rapid earthquake source products: magnitude and location estimates, CMT solutions, finite fault slip inversions, regional moment tensors, and fully heterogeneous slip inversions. The strategy is to rapidly (within a few minutes) produce an estimate of seafloor deformation from these earthquake source products and use it as the initial condition in tsunami propagation modeling.

2.1. Earthquake Source Products

To demonstrate the performance of this approach, we focus on the most rapidly available source information: rapid location estimates from seismic stations and magnitude estimates potentially available from coastal seismic and GPS stations (Figure 2) [*Melgar et al*., 2015]. For the Maule, Tohoku-oki, and Iquique events we rely on scaling relationships based on a growing earthquake catalog (*M*6–*M*9) of measurements of peak ground displacement (PGD) at coastal GPS stations to determine event magnitude [*Melgar et al*., 2015]. PGD scaling has been demonstrated to provide moment magnitude estimates with an uncertainty of 0.3 magnitude units within the first 1–2 min of origin time for these three events, depending on the earthquake size and station geometry. For the M_w8.3 Illapel earthquake, the magnitude based on PGD scaling is estimated to be M_w8.0 (Table 1, Figure S2). The advantage of using GPS-estimated PGD magnitude compared to only seismic data is that it does not saturate for very large earthquakes [*Melgar et al*., 2015]. The GPS positions were estimated for all four events in a simulated real-time mode by precise point positioning with ambiguity resolution [*Geng et al*., 2013]. We also highlight the performance of a rapid geodetic source size and slip estimates demonstrated for the M_w9.0 Tohoku-oki earthquake [*Colombelli et al*., 2013]. This method uses static offset data to fit a small number of large (50×90 km) fault patches with the strike and dip of a predefined slab model. It has the added advantage of rapidly estimating fault length in addition to magnitude. We choose to use these approaches for rapid magnitude estimation, but other methods exist and are being developed for both earthquake and tsunami warning [e.g., *Ohta et al*., 2012; *Melgar et al*., 2013; *Grapenthin et al*., 2014; *Minson et al*., 2014].

We assume a predefined slab model [*Hayes et al*., 2012]. Once a magnitude is known from the PGD scaling relationship (or from any other regional source products such as a CMT solution), we use another scaling relationship [*Blaser et al*., 2010] to estimate the dimensions of fault rupture, width (W), and length (L):

$$\begin{aligned} \log10(L) &= -2.37 + 0.57 \times Mw \\ \log10(W) &= -1.86 + 0.46 \times Mw. \end{aligned} \tag{1}$$

This scaling relationship is based on an analysis of a historical catalog of finite fault models of subduction zone events.

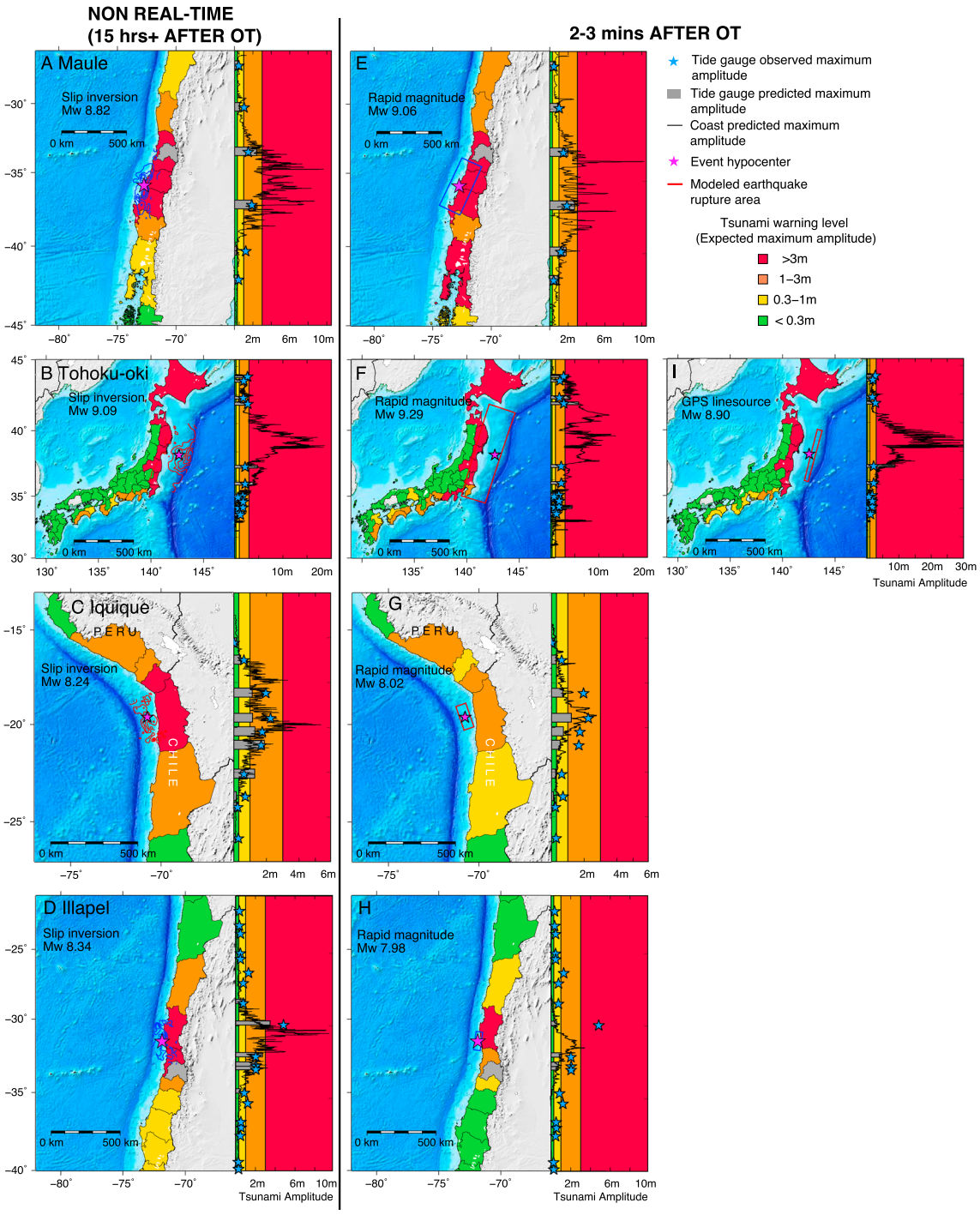

Figure 2. Tsunami warning maps and coastline amplitude predictions. (a) The 2010 Maule, Chile, (b) 2011 Tohoku-oki, Japan, (c) the 2014 M_w8.24 Iquique, Chile, and (d) the 2015 M_w8.34 Illapel, Chile, earthquakes. Figures 2a–2d show warning levels for each event from the joint slip inversion of ocean- and land-based data. These maps are calculated with a fine-scale coastline, and computation takes on the order of tens of hours. They are used as a baseline for comparison of the performance of the rapid source products but cannot be generated in real time. Magenta stars are the event epicenters. Red or blue contours are the observed pattern of slip (Figures S3–S6). Next to each warning map are the tsunami amplitude predictions at the coastline at 1 km intervals (black curves). The blue stars are the observed maximum amplitudes at tide gauges (TG) and the grey bars the prediction from the tsunami model at the tide gauge locations. (e–h) Warning maps and amplitude curves from the rapid magnitude tsunami models. (i) Warning maps and amplitude curves from the rapid geodetic source inversion [*Colombelli et al.*, 2013] (Figure S4c). For the rapid magnitude models, red or blue rectangles represent the inferred source size from scaling laws [*Blaser et al.*, 2010]. Additionally, for these models, amplitude curves are calculated at 1 km intervals on coarse coastlines and are computed in less than 2 min (Figure S1).

Table 1. Sensors Available for Each Earthquake

Earthquake	High-Rate GPS[a]	Strong Motion	Wave Gauge	Tide Gauge
M_w8.8 2010 Maule, Chile	8	-	-	2
M_w9.0 2011 Tohoku-oki, Japan[b]	20	20	6[c]	-
M_w8.2 2014 Iquique, Chile	8	15	-	4
M_w8.3 2015 Illapel, Chile	9	9	-	8

[a]1 Hz sampling rate.
[b]Slip model from *Melgar and Bock* [2015].
[c]Two ocean bottom pressure gauges and four GPS tsunami buoys.

After the fault dimensions are calculated, we place sufficient slip on the fault to match the scalar moment, using a uniform rigidity value of 45 GPa. For the rapid PGD magnitude model, we use the strike and dip of the predefined slab model at the hypocenter. For the moment tensor, we use the strike and dip from the nodal plane solution. These source products are all available within 1–2 min of rupture initiation [*Colombelli et al*., 2013; *Melgar et al*., 2015]. The performance of regional CMT solutions, potentially available in the first 2–5 min [*Guilhem et al*., 2013; *Melgar et al*., 2013], is tested as well (Figure S3).

As a baseline for comparison to our simplified approach for obtaining source parameters, we also use kinematic slip inversions from joint inversions of onshore and offshore data. We use the MudPy multitime window inversion code [*Melgar and Bock*, 2015]. The slip inversions and station distributions are shown in Figures S4–S7. Each event has different types and quantities of station data available (Table 1). We used 3-D surfaces for the fault geometry obtained from the Slab 1.0 model of global subduction zones [*Hayes et al*., 2012] for all events. Data fits for the Maule, Iquique, and Illapel inversions are shown in Figures S8–S10. Data fits for the Tohoku-oki inversion are in the original publication [*Melgar and Bock*, 2015].

2.2. Tsunami Modeling

The simplified approach requires some preparatory work for a particular plate boundary of interest. The slab geometry is partitioned into 10×10 km subfaults and a set of elastic deformation Green's functions are precomputed that relate unit slip on each subfault to the deformation of the seafloor on a regular grid spaced at 0.05° in latitude and longitude covering the source area. Once the earthquake source is rapidly characterized, the multiplication of the vector containing the computed slip on each subfault and the Green's functions matrix yields the expected deformation at each grid node on the seafloor. We calculate not just the vertical deformation but also the horizontal motion at each node predicted by the source model. This allows us to account for horizontal advection of steep bathymetry [*Bletery et al*., 2015; *Melgar and Bock*, 2015], which can increase the tsunami amplitude. These seafloor motions are then used as the initial conditions for tsunami modeling. At this modeling stage we use a nonlinear shallow water propagation code [*LeVeque et al*., 2011] from which we obtain tsunami coastal amplitude curves, i.e., the maximum expected tsunami, at 1 km intervals along the local coastline (Figure 2). Note that we do not use precomputed tsunami Green's functions at this step; rather, we model the fully nonlinear wave propagation.

In order to determine whether the tsunami coastal amplitude curves derived from rapid earthquake source products compare favorably with the actual tsunami, we establish a baseline to compare against. For this "ground truth," we use the tsunami models derived from the fully heterogeneous joint slip inversions of land- and ocean-based data (Figures 2a–2d). It is reasonable to use these models because they compare favorably with postevent tsunami survey measurements (Figure S11). This approach provides a high-resolution ground truth against which to judge the more timely and simplified approaches, but importantly, it also provides estimates of the tsunami where there are no direct measurements from tide gauges. To put this in perspective for effective tsunami warning, direct tide gauge readings are typically not available until 15–60 min after earthquake origin time.

It is important to note that in order to make the rapid tsunami models of Figures 2e–2i, we have made a critical simplification. The simulations that use the joint ocean- and land-based sensor slip inversion use the best publicly available topography and bathymetry data sets. Onshore topography is 90 m pixels from the Shuttle Radar Topography Mission (SRTM) 3 data set [*Sandwell and Smith*, 2009] and bathymetry are 1 km pixels from the SRTM30+ data set [*Farr et al*., 2007]. For the rapid magnitude and moment tensor computations, we use only the SRTM30+ data set and disregard the more detailed onshore topography. Using only the coarse bathymetry and topography speeds up the tsunami computation from the order of tens of hours to less than

Table 2. Comparison of Earthquake Magnitude Estimates

Earthquake	Final[a] M_w	Inversion[b] M_w	Rapid[c] M_w
2010 Maule, Chile	8.8	8.82	9.06
2011 Tohoku-oki, Japan	9.0	9.09	9.29
2014 Iquique, Chile	8.2	8.24	8.02
2015 Illapel, Chile	8.3	8.32	7.98

[a]http://earthquake.usgs.gov/.
[b]Slip inversion (Figures 2 and S4–S7).
[c]PGD scaling relationship [*Melgar et al*., 2015].

2 min (Figure S1) for all tested events. There exist semianalytical approaches for runup computation that do not require complex numerical calculation and could reduce the warning time even further but also reduce the complexity of tsunami propagation that can be modeled [*Riquelme et al*., 2015].

2.3. Tsunami Warning Maps

The tsunami amplitude curves (Figure 2) are not directly useful for warning the general population; they are too complex. Instead, we mimic the approach taken by the JMA system that issues warnings at the administrative level 1, which in Japan corresponds to prefectures and in Chile to regions. Thus, if any point along the coast of a particular prefecture or region exceeds one of the predefined amplitude thresholds, the whole region is color coded accordingly. These warning maps use the following standard warning levels: 0–0.3 m, 0.3–1 m, 1–3 m, and 3m or more and receive the corresponding color codes (green, yellow, orange, and red). These levels correspond to small, moderate, large, and major tsunamis, respectively, based on the potential for infrastructure damage and loss of life. Other simple qualitative levels are used for tsunami warnings. In Japan, for example, the levels are referred to as tsunami advisory, tsunami warning, and large tsunami warning; in Australia, the warning levels are no threat, marine threat, and land threat [*Allen and Greenslade*, 2008]. Irrespective of the warning heuristics chosen, we note that the aggregate of the rapid earthquake source estimate plus tsunami modeling times means our approach to elaborating warning maps can deliver results in minutes.

3. Results

To assess the accuracy and utility of our approach, we compare the tsunami amplitudes based only on the rapid magnitude estimates to the amplitudes observed at the few local tide gauges (Figure 2) and find good agreement. As a further assessment, we compare our rapid tsunami amplitudes to the baseline tsunami amplitude curves estimated through a more rigorous, but less timely, earthquake slip inversion as discussed in section 2.

The rapid magnitude calculations are within the magnitude uncertainty of ±0.3 magnitude units [*Melgar et al*., 2015] for all considered earthquakes (Table 2). Applying the scaling relationship (equation (1)) relating magnitude to fault size yields fault dimensions different from the actual observed pattern of slip. Correspondingly, the tsunami amplitude curves are not as accurate (compare the tide gauge observations and predictions). The effects of these errors in the rapid magnitude estimates are particularly obvious for the 2011 Tohoku-oki event; the fault length from the PGD magnitude is longer than the more compact observed pattern of slip, impacting the coastal amplitude curves and leading to overpredictions of amplitude to the north and south of the rupture area where there is spurious slip. Similarly, in the Iquique Illapel events, the smaller source size as estimated from the PGD magnitude leads to an overall underprediction of the maximum amplitude. This is particularly evident for the Illapel event.

4. Discussion

In spite of variations in the details of the tsunami amplitude introduced by imperfect source information, there are only minor differences in the warning maps produced at the region and prefecture level. Furthermore, the warning maps based on rapid magnitude estimates are available in the first 1–2 min after earthquake origin time and require less than two additional minutes of computation time (Figure S1). The result is rapid actionable information on expected tsunami heights, otherwise not widely available for local tsunamis. To prompt evacuations, the high spatial resolution of the tsunami amplitude curves is unnecessary; decision makers are provided with the region and prefecture level maps. Thus, the loss of precision that results from the modeling assumptions used in the most rapid estimate is acceptable, while the simplifications allow for rapid local warnings.

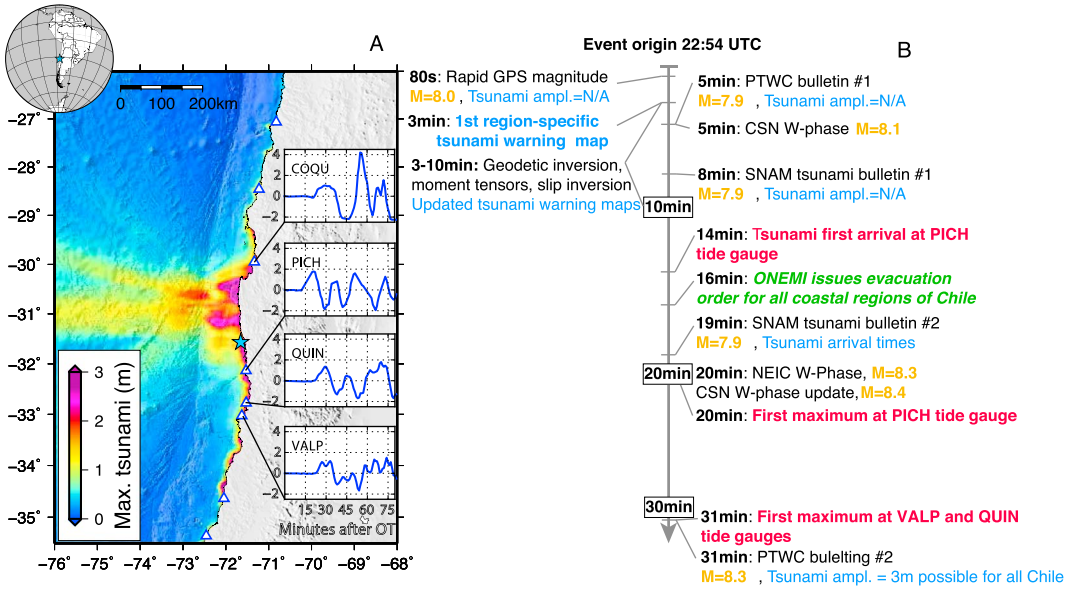

Figure 3. Maximum tsunami amplitude and timeline of events for the 2015 M_w8.3 Illapel earthquake. (a) The maximum amplitudes are those predicted by the joint inversion of GPS, strong motion, and tide gauge data (Figure S6b) and is the same as that used in Figure 2d to generate the coastal amplitude curves. The insets are 75 min of tide gauge records at the closest sties after removing tides and relative to the earthquake origin time. The amplitudes are in meters above nominal sea level. (b) Timeline of events, on the left-hand side is what would be achievable with the approach proposed here; on the right are the determinations of national and international agencies. PTWC is the Pacific Tsunami Warning Center from the United States, CSN the Centro Sismológico Nacional of Chile, SNAM is the Sistema Nacional de Alerta de Maremotos of Chile, ONEMI is the Oficina Nacional de Emergencia del Ministerio del Interior of Chile, and NEIC is that National Earthquake Information Center from the United States.

Not all large earthquakes in subduction zones occur on the megathrust. Outer rise normal faulting events [*Okal et al.*, 2010] and strike-slip events [*Hill et al.*, 2015] are possible and can lead to errors in the warnings issued [*Lauterjung et al.*, 2014]. However, for subduction zones the thrust event assumption is reasonable, especially when only minutes are available to issue a warning. At such short time scales, it is the only course of action. As the event unfolds, and as we have demonstrated here, more elaborate source products such as line source CMT solutions [*Melgar et al.*, 2013] can be used in the same way, providing ever better estimates of tsunami amplitude and better matching the results (Figures 2a–2d). For example, rapid geodetic estimates of fault dimension and slip [*Colombelli et al.*, 2013; *Melgar et al.*, 2013; *Grapenthin et al.*, 2014] can better determine the geographic extent of the tsunami (Figure 2i). These approaches are advantageous especially in situations where the actual source dimension deviates from what is predicted by the scaling laws of *Blasser et al.* [2010]. The Tohoku-oki event is a good example. The fault length is shorter (~400 km) than what is predicted by the scaling laws for an M_w9.0–9.1 event (~600 km). Regional moment tensors confirm (or change) the style of faulting assumed and the fault geometry (Figure S3), and slip inversions can better constrain the heterogeneity of slip. Such products are delayed anywhere from tens of seconds to tens of minutes [*Dreger et al.*, 2005; *Duputel et al.*, 2011; *Grapenthin et al.*, 2014] after the rapid magnitude estimates become available. There is thus a trade-off between latency and accuracy. A cascading system for local tsunami warning is desirable: first, from rapid magnitude estimates, then refinements from improved source products, followed by direct measurements at nearshore wave gauges, tide gauges, and ocean-basin sensors such as DART buoys. At each stage, the tsunami warning can be refined for more accurate estimates of the expected extent of inundation and as a guide for rapid response by emergency responders and decision makers.

In this context, and to understand the potential impact of this work, it is demonstrative to review the actual timeline of events during the recent 2015 M_w8.3 Illapel earthquake and tsunami (Figure 3). Tsunami first arrivals where registered at 14 min after observation time (OT) at the closest tide gauges and the first peak amplitudes where achieved between 20 and 31 min after OT. The Chilean National Emergency Management Office (ONEMI) issued an evacuation notice at 16 min after OT for all the coastal areas of Chile; this eventually led to an evacuation of 1 million people. The warnings were based on the earthquake magnitudes estimated by the

Pacific Tsunami Warning center (PTWC, M_w7.9) and the Centro Sismológico Nacional (CSN, M_w8.1). There was no information on the forecast tsunami intensity when the evacuation was ordered. The first forecasts were made in the second PTWC bulletin at 31 min after OT (Figure 3b) based on an M_w8.3 point source, forecasting 3 m of possible amplitude for selected regions of Chile. In contrast, the approach that we propose, using already available stations in Chile, could have produced a reliable magnitude (M_w8.0 ± 0.3) in the first 2 min with estimates of maximum expected tsunami amplitudes for each region well before 5 min after OT with rapid updates, thereafter (Figure 3b). Ostensibly, this would lead to better informed evacuation notices, tailored to specific regions of the affected area.

Direct measurements of the tsunami waves from offshore data on the continental shelf at intermediate water depths, close to, or directly above the earthquake would also improve the accuracy of the tsunami estimates. As opposed to tide gauges, these measurements make joint inversions possible and have been shown to be the most reliable source of information for precise warning and can provide actionable data before the tsunami strikes the local coastline [*Melgar and Bock*, 2013, 2015; *Tsushima et al*., 2014]. However, these sensors are much more expensive than land-based geophysical instruments due to the high deployment and maintenance costs. Our approach is simple and practical because land-based sensors exist in large numbers today, while offshore instrumentation on the continental slope is very rare. Furthermore, most countries along a subduction zone already have national monitoring agencies, which manage these stations and produce some form of rapid source product. These agencies are mandated to issue hazard warnings to governments and civil societies. Our results argue that these agencies could easily implement our approach and integrate it with their existing tsunami warning systems.

It is important to note that magnitude saturation, the systematic underestimation of events at magnitude larger than 7.5–8, is the most critical problem with systems relying on seismic instruments only. Magnitude saturation can lead to gross underprediction of tsunami amplitudes; indeed, this was the case during the 2011 M_w9.0 Tohoku-oki event that from seismic data alone was initially estimated at M_w7.9 leading the Japan tsunami warning system to issue amplitude forecasts that were far too low [*Hoshiba and Ozaki*, 2014]. Geodetic and seismic techniques that avoid saturation such as seismogeodesy [*Bock et al*., 2011] should be given a high priority. We posit that network operators can begin to incorporate tsunami warning into their toolkit immediately. As monitoring infrastructure grows and improves, and real-time source characterization algorithms become widely available for both earthquake and tsunami warning, they can be folded into our proposed cascading framework for real-time local tsunami warnings.

5. Conclusions

By leveraging source information from regional GPS and seismic networks, we have demonstrated the potential speedup in tsunami intensity estimation at the local coastlines adjacent to large events. Rapid magnitude estimates and more elaborate source products such as moment tensors and finite fault models can be used as the initial condition for fully nonlinear rapid tsunami models that can be computed within 2 min. A detailed analysis of the recent M_w8.3 Illapel, Chile, earthquake demonstrated that in the first 5 min substantially improved information on the expected intensity of the tsunami could have been available, potentially providing improved situational awareness for government agencies and likely a reduction in casualties.

Acknowledgments
This research was funded by the Gordon and Betty Moore Foundation through grant GBMF3024 to UC Berkeley. Participation at Scripps Institution of Oceanography was funded by NASA grants NNX12AH55G and NNX13AI45A-001 and NSF grants EAR-1252186 (EarthScope) and EAR-1252187. This work received partial support from grants ANR-2011-BS56-017 and ANR-2012-BS06-004 of the French Agence Nationale de la Recherche (ANR). We thank Barry Hirshorn and Lt. Nicolas Guzmán for helpful discussions on the timeline of warnings for the Illapel event. We also thank Randy LeVeque and Kyle Mandli for helpful discussions on the Geoclaw software. We also thank the Franco-Chilean international laboratory Montessus deBallore (LIA-MdB) for providing some of the Chilean high-rate GPS data.

References

Allen, R. M., P. Gasparini, O. Kamigaichi, and M. Böse (2009), The status of earthquake early warning around the world: An introductory overview, *Seismol. Res. Lett.*, *80*, 682–693.

Allen, S. C. R., and D. J. M. Greenslade (2008), Developing tsunami warnings from numerical model output, *Nat. Hazards*, *46*(1), 35–52.

Athukorala, P., and B. P. Resosudarmo (2005), The Indian Ocean tsunami: Economic impact, disaster management, and lessons, *Asian Econ. Pap.*, *4*, 1–39.

Blaser, L., F. Krüger, M. Ohrnberger, and F. Scherbaum (2010), Scaling relations of earthquake source parameter estimates with special focus on subduction environment, *Bull. Seismol. Soc. Am.*, *100*, 2914–2926.

Bletery, Q., A. Sladen, B. Delouis, and L. Mattéo (2015), Quantification of tsunami bathymetry effect on finite fault slip inversion, *Pure Appl. Geophys.*, *172*(12), doi:10.1007/s00024-015-1113-y.

Bock, Y., D. Melgar, and B. W. Crowell (2011), Real-time strong-motion broadband displacements from collocated GPS and accelerometers, *Bull. Seismol. Soc. Am.*, *101*, 2904–2925.

Center for International Earth Science Information Network (CIESIN) and Centro Internacional de Agricultura Tropical (CIAT) (2005), *Gridded Population of the World, Version 3 (GPWv3): Population Grids (SEDAC*, Columbia Univ., New York. [Available at http://sedac.ciesin.columbia.edu/gpw.]

Colombelli, S., R. M. Allen, and A. Zollo (2013), Application of real-time GPS to earthquake early warning in subduction and strike-slip environments, *J. Geophys. Res. Solid Earth*, *118*, 3448–3461, doi:10.1002/jgrb.50242.

Dreger, D. S., L. Gee, P. Lombard, M. H. Murray, and B. Romanowicz (2005), Rapid finite-source analysis and near-fault strong ground motions: Application to the 2003 M_w 6.5 San Simeon and 2004 M_w 6.0 Parkfield earthquakes, *Seismol. Res. Lett.*, *76*, 40–48.

Duputel, Z., L. Rivera, H. Kanamori, G. P. Hayes, B. Hirshorn, and S. Weinstein (2011), Real-time *W* phase inversion during the 2011 off the Pacific coast of Tohoku earthquake, *Earth Planets Space*, *63*(7), 535–539.

Farr, T. G., et al. (2007), The shuttle radar topography mission, *Rev. Geophys.*, *45*, RG2004, doi:10.1029/2005RG000183.

Geng, J., Y. Bock, D. Melgar, B. W. Crowell, and J. S. Haase (2013), A new seismogeodetic approach applied to GPS and accelerometer observations of the 2012 Brawley seismic swarm: Implications for earthquake early warning, *Geochem. Geophys. Geosyst.*, *14*, 2124–2142, doi:10.1002/ggge.20144.

Grapenthin, R., I. A. Johanson, and R. M. Allen (2014), Operational real-time GPS-enhanced earthquake early warning, *J. Geophys. Res. Solid Earth*, *119*, 7944–7965, doi:10.1002/2014JB011400.

Guilhem, A., D. S. Dreger, H. Tsuruoka, and H. Kawakatsu (2013), Moment tensors for rapid characterization of megathrust earthquakes: The example of the 2011 M 9 Tohoku-oki, Japan earthquake, *Geophys. J. Int.*, *192*, 759–772.

Hayes, G. P., P. S. Earle, H. M. Benz, D. J. Wald, and D. J. Briggs (2011), 88 Hours: The US geological survey national earthquake information center response to the 11 March 2011 M_w 9.0 Tohoku earthquake, *Seismol. Res. Lett.*, *82*, 481–493.

Hayes, G. P., D. L. Wald, and R. L. Johnson (2012), Slab1.0: A three-dimensional model of global subduction zone geometries, *J. Geophys. Res.*, *117*, B01302, doi:10.1029/2011JB008524.

Hill, E. M., et al. (2015), The 2012 M_w 8.6 Wharton Basin sequence: A cascade of great earthquakes generated by near-orthogonal, young, oceanic mantle faults, *J. Geophys. Res. Solid Earth*, *120*, 3723–3747, doi:10.1002/2014JB011703.

Hirshorn, B., S. Weinstein, and S. Tsuboi (2013), On the application of M_{wp} in the near field and the March 11, 2011 Tohoku earthquake, *Pure Appl. Geophys.*, *170*, 975–991.

Hoshiba, M., and T. Ozaki (2014), Earthquake early warning and tsunami warning of the Japan Meteorological Agency, and their performance in the 2011 off the Pacific Coast of Tohoku Earthquake (M_w 9.0), in *Early Warning for Geological Disasters*, pp. 1–28, Springer, Berlin.

Kumar, S. T., et al. (2012), Performance of the tsunami forecast system for the Indian Ocean, *Curr. Sci.*, *102*(1), 110–114.

Lauterjung, J., A. Rudloff, U. Münch, and D. J. Acksel (2014), The earthquake and tsunami early warning system for the Indian Ocean (GITEWS), in *Early Warning for Geological Disasters*, pp. 165–178, Springer, Berlin Heidelberg.

LeVeque, R. J., D. L. George, and M. J. Berger (2011), Tsunami modeling with adaptively refined finite volume methods, *Acta Numer.*, *20*, 211–289.

Melgar, D., and Y. Bock (2013), Near-field tsunami models with rapid earthquake source inversions from land- and ocean-based observations: The potential for forecast and warning, *J. Geophys. Res. Solid Earth*, *118*, 5939–5955, doi:10.1002/2013JB010506.

Melgar, D., and Y. Bock (2015), Kinematic earthquake source inversion and tsunami runup prediction with regional geophysical data, *J. Geophys. Res. Solid Earth*, *120*, 3324–3349, doi:10.1002/2014JB011832.

Melgar, D., B. W. Crowell, Y. Bock, and J. S. Haase (2013), Rapid modeling of the 2011 M_w 9.0 Tohoku-oki earthquake with seismogeodesy, *Geophys. Res. Lett.*, *40*, 2963–2968, doi:10.1002/grl.50590.

Melgar, D., et al. (2015), Earthquake magnitude calculation without saturation from the scaling of peak ground displacement, *Geophys. Res. Lett.*, *42*, 5197–5205, doi:10.1002/2015GL064278.

Mimura, N., K. Yasuhara, S. Kawagoe, H. Yokoki, and S. Kazama (2011), Damage from the Great East Japan earthquake and tsunami—A quick report, *Mitigation Adapt. Strategies Global Change*, *16*, 803–818.

Minson, S. E., J. R. Murray, J. O. Langbein, and J. S. Gomberg (2014), Real-time inversions for finite fault-slip models and rupture geometry based on high-rate GPS data, *J. Geophys. Res. Solid Earth*, *119*, 3201–3231, doi:10.1002/2013JB010622.

Ohta, Y., et al. (2012), Quasi real-time fault model estimation for near-field tsunami forecasting based on RTK-GPS analysis: Application to the 2011 Tohoku-oki Earthquake (Mw 9.0), *J. Geophys. Res.*, *117*, B02311, doi:10.1029/2011JB008750.

Okal, E., et al. (2010), Field survey of the Samoa tsunami of 29 September 2009, *Seismol. Res. Lett.*, *81*, 577–591.

Riquelme, S., M. Fuentes, G. P. Hayes, and J. Campos (2015), A rapid estimation of near field tsunami runup, *J. Geophys. Res. Solid Earth*, *120*, 6487–6500, doi:10.1002/2015JB012218.

Sandwell, D. T., and W. H. F. Smith (2009), Global marine gravity from retracked Geosat and ERS-1 altimetry: Ridge segmentation versus spreading rate, *J. Geophys. Res.*, *114*, B01411, doi:10.1029/2008JB006008.

Tatehata, H. (1997), The new tsunami warning system of the Japan Meteorological Agency, in *Perspectives on Tsunami Hazard Reduction*, pp. 175–188, Springer, Netherlands.

Titov, V. V., et al. (2005), Real-time tsunami forecasting: Challenges and solutions, in *Developing Tsunami-Resilient Communities*, pp. 41–58, Springer, Netherlands.

Tsushima, H., R. Hino, Y. Ohta, T. Iinuma, and S. Miura (2014), tFISH/RAPiD: Rapid improvement of near-field tsunami forecasting based on offshore tsunami data by incorporating onshore GPS data, *Geophys. Res. Lett.*, *41*, 3390–3397, doi:10.1002/2014GL059863.

Yun, N. Y., and M. Hamada (2015), Evacuation behavior and fatality rate during the 2011 Tohoku-Oki earthquake and tsunami, *Earthquake Spectra*, *31*(3), 1237–1265.